Received: 28 November 2022 | Revised: 24 April 2023 | Accepted: 27 April 2023

DOI: 10.1002/cne.25495

RESEARCH ARTICLE

JCN RESEARCH IN SYSTEMS NEUROSCIENCE THE JOURNAL OF COMPARATIVE NEUROLOGY WILEY

Central projections of auditory nerve fibers in the western rat snake (*Pantherophis obsoletus*)

Dawei Han[1,2] | **Catherine E. Carr**[1]

[1]Department of Biology, University of Maryland, College Park, Maryland, USA

[2]Neuroscience and Cognitive Science Program, University of Maryland, College Park, Maryland, USA

Correspondence
Catherine E. Carr, Department of Biology, University of Maryland, College Park, MD 20742, USA.
Email: cecarr@umd.edu

Funding information
National Institutes of Health, Grant/Award Number: R01DC019341

Abstract

Despite the absence of tympanic middle ears, snakes can hear. They are thought to primarily detect substrate vibration via connections between the lower jaw and the inner ear. We used the western rat snake (*Pantherophis obsoletus*) to determine how vibration is processed in the brain. We measured vibration-evoked potential recordings to reveal sensitivity to low-frequency vibrations. We then used tract tracing combined with immunohistochemistry and Nissl staining to describe the central projections of the papillar branch of the VIIIth nerve. Applications of biotinylated dextran amine to the basilar papilla (homologous to the organ of Corti of mammals) labeled bouton-like terminals in two first-order cochlear nuclei, a rostrolateral nucleus angularis (NA) and a caudomedial nucleus magnocellularis (NM). NA formed a distinct dorsal eminence, consisted of heterogenous cell types, and was parvalbumin positive. NM was smaller and poorly separated from the surrounding vestibular nuclei. NM was distinguished by positive calbindin label and included fusiform and round cells. Thus, the atympanate western rat snake shares similar first-order projections to tympanate reptiles. Auditory pathways may be used for detecting vibration, not only in snakes but also potentially in atympanate early tetrapods.

KEYWORDS
auditory, cochlear nerve, cochlear nuclei, immunohistochemistry, reptile, snake, tract tracing

1 | INTRODUCTION

With over 4000 species in the suborder Serpentes, snakes are a diverse group of reptiles that have invaded ecological niches ranging from the oceans to tropical canopies (Uetz et al., 2023). Little is known about their auditory systems, except that they lack tympana and are instead thought to detect vibration through the lower jaw (Wever, 1978), which articulates with the quadrate coupled to the inner ear via the stapes (Figure 1a). How snakes process this vibrational information is poorly understood, motivating our study of the auditory nerve projections to brain.

Among sauropsids, auditory brainstem circuitry has been most extensively studied in birds, and their organization is thought to be representative of all groups in this clade (Carr et al., 2016; Conlee & Parks, 1986; Takahashi & Konishi, 1988a, 1988b; Walton et al., 2017). The auditory branch of the VIIIth nerve terminates in two nuclei, a more caudal nucleus magnocellularis (NM) and a rostral nucleus angularis (NA). NM and NA serve as the first-order cochlear nuclei for ascending binaural and monaural pathways to the inferior colliculus (Ashida & Carr, 2011; Grothe et al., 2004).

Prior studies of the snake auditory system have shown that the auditory portion of the VIIIth nerve targets dorsal nuclei in the rostral

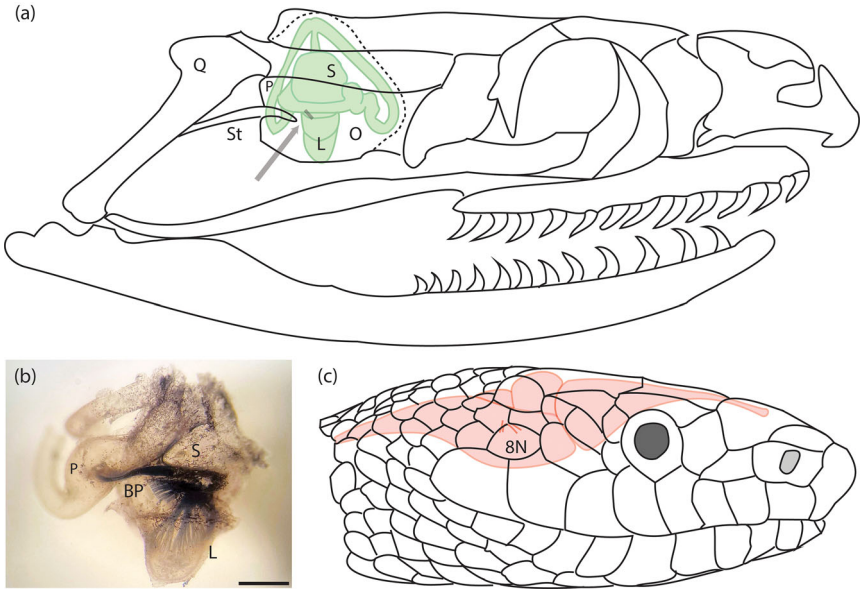

FIGURE 1 Overview of auditory structures of the western rat snake. (a) Schematic line drawing of the skull of the western rat snake showing the relative position of the inner ear (green). Rostral border of the otic capsule is marked by the dashed line. Gray arrow points to the basilar papilla located close to the medial wall of the membranous labyrinth. L, lagena; O, otic capsule; P, posterior semicircular canal; Q, quadrate; S, saccule; St, stapes. Line drawing of the rat snake skull was adapted from Auen and Langebartel (1977). (b) Medial view of the posterior branch of the VIIIth nerve innervating the basilar papilla (BP), lagena macula (L), and posterior crista (P). The nervous tissue was stained with Sudan black B. The saccular macula (S) is on the opposite side (lateral) and occluded from view. Scale bar = 1 mm. (c) Schematic line drawing of the head of the western rat snake and the relative position of the brain (pink). 8N, cranial nerve VIII.

medulla, although interpretation and description of its first-order projections vary. Holmes (1902) described a single "small and ill-defined" nucleus dorsalis. Weston (1936) described a single cochlear nucleus homologous to NA, while ten Donkelaar and Nieuwenhuys (1979) found only a "dorsal magnocellular nucleus." Schwab (1979) confirmed a single cochlear nucleus but noted that in *Cylindrophis* it could be divided into anterior and posterior subnuclei. Molenaar (1976), while examining *Python reticulatus*, identified a small rostral NA in addition to a large caudal NM. Miller (1980) also differentiated NM and NA, and further separated NM into nucleus magnocellular medialis and NM lateralis to align with the nuclear subdivisions of the caiman (Leake, 1974) but noted that in some species NA was not "sharply demarcated" and the two magnocellular nuclei may be merged. These results were agreed upon by DeFina (1981) and Defina and Kennedy (1983).

There are several potential explanations for the inconsistencies in the description of snake cochlear nuclei. First, most literature recognized snake cochlear nuclei based on histological boundaries, which may be confounded when nuclei lack differentiation, a phenomenon sometimes observed in the octavolateralis system (McCormick, 1999). Second, snakes in general have small basilar papillae (Miller, 1968, 1978; Wever, 1978). In vivo recordings show auditory sensitivities below 1000 Hz, which is a restricted low-frequency bandwidth compared with most other sauropsids (Christensen et al., 2012; Hartline, 1971; Wever, 1978), suggesting that snake cochlear nuclei may be reduced and potentially difficult to find. Third, snakes lack a tympanum and are therefore most sensitive to substrate vibration (Hartline, 1971; Hartline & Campbell, 1969; Wever, 1978). They detect high-amplitude sound pressure via sound-induced head vibrations (Christensen et al., 2012).

In this study, we used tract tracing, immunohistochemistry, and Nissl staining to investigate the projections of the cochlear branch of the VIIIth nerve in the western rat snake (*Pantherophis obsoletus*). We hypothesized that there are dedicated auditory nuclei in the brainstem similar to that seen in other sauropsids and that inconsistencies in the literature might reflect species-specific variation. The western rat snake was selected due to its wide availability, indications of distinct cochlear nuclei (DeFina, 1981; Defina & Kennedy, 1983), moderate hearing abilities (Wever, 1978), and well-described inner ear (Miller & Beck, 1990). In addition, Wever's (1978) methods of using cochlear microphonics to assess hearing thresholds have received criticism (Manley, 2017), so we re-evaluated auditory sensitivity of the western rat snake using vibration-evoked potential recordings. We found the western rat snake was most sensitive to low frequencies, similar to other snakes. Further, we showed that the auditory nerve of the western rat snake projects to two first-order cochlear nuclei, a small caudomedial NM and a larger, distinct rostrolateral NA.

2 | MATERIAL AND METHODS

A total of 37 western rat snakes (*P. obsoletus*; snout–vent length: 20–140 cm) were obtained commercially for this study. Snakes were kept in a 12:12-h light–dark cycle with 21–27°C temperature range and offered mice and water ad libitum. Anesthesia and animal handling protocols were approved by the University of Maryland College Park Animal Care and Use Committee.

2.1 | Vibration-evoked potential recordings

Twelve snakes were used for vibration-evoked potential recordings. Snakes were anesthetized with isoflurane (5%) until fully anesthetized (determined by loss of muscle tone, lack of righting reflex, and lack of reflex to tail pinch), and plane of anesthesia was maintained with 2% isoflurane for the duration of the experiment. Experiments were performed in an anechoic chamber (21°C). We used QuickABR, a custom software developed by Christian Brandt (University of Southern Denmark, Odense, Denmark), to generate stimuli and record evoked

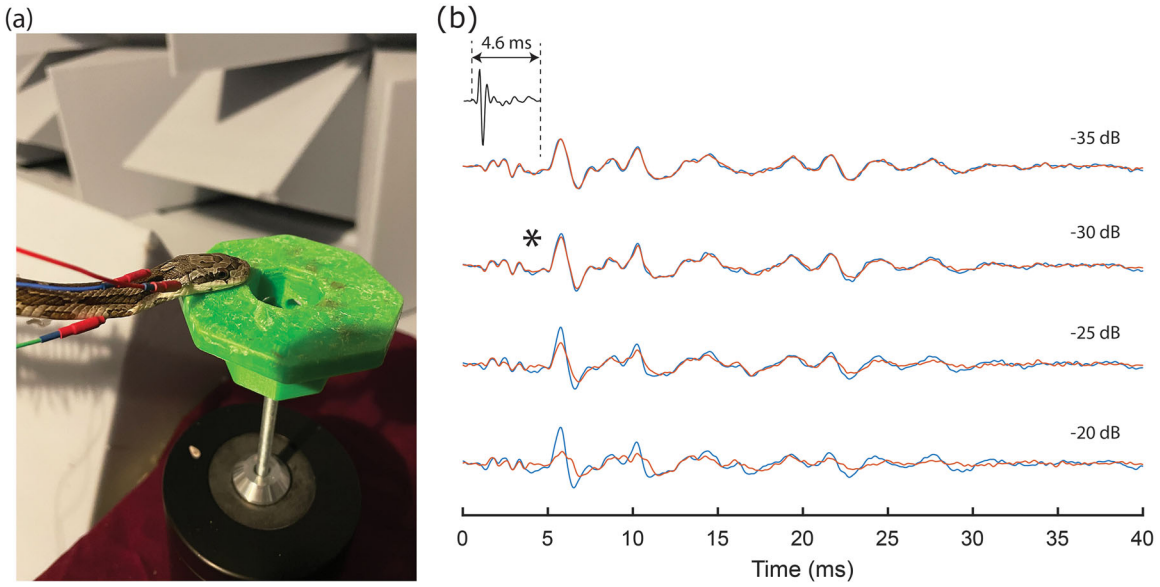

FIGURE 2 Vibration-evoked potential recordings. (a) Recording setup for measuring evoked potentials. The snake's head was placed on the green platform connected to a mini shaker. Two recording electrodes were inserted on the snake's head, one dorsal to the brainstem (blue) and one dorsal to the VIIIth nerve (red). The reference electrode (green) was inserted into the neck of the snake. (b) Vibration-evoked potential waveforms in response to click stimulations in the presence of a 100-Hz masker. Responses to masked (orange) and unmasked (blue) clicks were overlaid, and threshold was determined visually as the lowest level where a clear discriminable difference could be seen from the two waveforms (indicated by the asterisk). Click stimulus is shown above evoked potential waveforms in black

potentials (Brandt et al., 2007). Vibrational stimuli were produced with a mini-shaker (Type 4810; Brüel & Kjær, Nærum, Denmark) connected to a custom-made platform and placed under the snake's head (Figure 2a; Christensen et al., 2012). The mini-shaker was calibrated using a piezoelectric accelerometer (Type 4381; Brüel & Kjær, Nærum, Denmark) connected to a conditioning amplifier (Type 1704; Brüel & Kjær). The accelerometer itself was calibrated using a calibration exciter (Type 4294; Brüel & Kjær) at 10 ms^{-2}, 159.15 Hz.

Vibrational stimuli and experimental procedure for measuring vibration-evoked potential recordings followed that of Capshaw et al. (2020). In brief, we compared evoked potentials in response to a broadband click with or without a masking tone, and detection thresholds were determined visually as the lowest level where the tone had a masking effect (Figure 2b). Compared to using tone bursts, this method avoids the "frequency splatter" of short low-frequency stimuli (Brandt et al., 2018). The click stimulus used consisted of one half cycle of a 2000-Hz signal at an amplitude that elicited 90% of the maximal neural response, and pure tone maskers ranged from 20 to 1000 Hz. Three electrodes were inserted subcutaneously, including two measuring electrodes, one dorsal to the brainstem and one dorsal to the VIIIth cranial nerve, and one reference electrode placed into the neck of the snake (Figure 2a). Evoked potentials were amplified with an RA4PA Medusa pre-amplifier (Tucker Davis Technologies, Alachua, FL, USA) and recorded by an RM2 digital signal processor (Tucker Davis Technologies, Alachua, FL, USA) with a sampling rate of 24.4 kHz. Evoked potentials were averaged over 800 repetitions, and every second stimulus was phase inverted. Vibration thresholds were plotted against frequency in MATLAB v2019b (Mathworks, Natick, MA, USA).

2.2 | Tract tracing

A total of 19 snakes were used for tract tracing. Following the anesthesia described above, the heart was exposed by ventrally opening the body cavity, and the snakes were perfused transcardially with oxygenated ice-cold Ringer's solution (96.5 mM NaCl, 31.5 mM $NaHCO_3$, 4 mM $CaCl_2$, 2.6 mM KCl, 2 mM $MgCl_2$, and 20 mM D-glucose, from Kohl et al. [2014]). After decapitation and removal of the lower jaw, the dorsal skull was placed in a Sylgard-lined dish containing ice-cold Ringer's solution.

To locate the auditory endorgan, the basilar papilla, and its associated nerve bundle in the inner ear labyrinth, we first stained the inner ear with Sudan black B, modified from procedures of Rasmussen (1961). Briefly, the whole head was immersion-fixed in 4% paraformaldehyde in 0.01 M phosphate-buffered saline (PBS) overnight. The membranous labyrinth of the inner ear was carefully dissected out and washed in distilled water to remove excess fixative. The tissue was rinsed in 30%, 50%, and 70% ethanol for 5 min each, then transferred to a saturated alcoholic solution of Sudan black B. After staining for 10 min, the tissue was transferred to 70% ethanol for differentiation under the dissection scope, then washed in 50% ethanol and distilled water. Finally, the tissue was transferred to 90% glycerol for clearing and storage.

To label afferents from the basilar papilla, the otic capsule was opened dorsally to expose the membranous labyrinth. After removal of otoconia in the saccule, the saccular macula was moved aside, and the cochlear duct opened with fine forceps to reveal the small bundle of nerves supplying the basilar papilla. Excess fluids were removed, and biotinylated dextran amine (BDA; Dextran, Biotin, 3000MW, Lysine Fixable, Invitrogen, Carlsbad, CA, USA) crystals were applied to the papillar nerve bundle with a tungsten electrode. The isolated head was placed in a humid chamber in an 8–10°C refrigerator to allow tracer uptake for 15 min, and then rinsed multiple times with Ringer's solution to remove excess tracer.

After injection of tracer into the basilar papilla, the isolated head was immersed in oxygenated Ringer's solution in an 8–10°C refrigerator for 24–48 h to allow for tracer transport, with oxygenated Ringer's solution changed every 12–24 h. The brain was then immersion-fixed in 4% paraformaldehyde in 0.01 M PBS for 24 h, and subsequently cryoprotected in 30% sucrose in 0.01 M PBS for 24 h. Tissue was cut on a freezing microtome in 50-μm coronal sections, rinsed in 0.01 M PBS, and then incubated in avidin biotin complex (ABC; Vector Laboratories, Burlingame, CA, USA), in 0.2% Triton X in 0.01 M PBS solution for 12 h at room temperature. Afterward, sections were reacted using Vector SG/Peroxidase Substrate Kit (Vector Laboratories) for 5–10 min, rinsed with buffer, and then mounted on gelatin-subbed slides. After air-drying overnight, slides were counterstained with Neutral Red, dehydrated, and cover slipped. In specimens used for basilar papillae label, the membranous labyrinths were also dissected free, reacted, and mounted to check for possible contamination of tracer in other endorgans.

2.3 | Immunohistochemistry

A total of three snakes were used for immunohistochemistry studies. After fixing and cryoprotecting the brain as described above, the brains were sectioned on a freezing microtome at 30-μm coronal sections. Free-floating sections were incubated in a blocking solution of 4% normal goat serum in 0.01 M PBS with 0.4% Triton-X (TX) for 20 min. Sections were subsequently incubated in antisera against (1) calbindin (CB; Swant, Belinzona, Switzerland; Cat# CB38, RRID: AB_10000340) and (2) parvalbumin (PV; Sigma–Aldrich, St. Louis, MO, USA; Cat# ZRB1218, RRID: AB_2893272), both diluted at 1:1000 in 0.01 M PBS and 0.02% TX, for 18 h at 4°C (Yan et al., 2010). After washing, sections were incubated in biotinylated goat anti-rabbit secondary antisera (Vector Laboratories; Cat# BA-1000, RRID: AB_2313606), diluted at 1:1000 in 0.01 M PBS and 0.02% Triton-X, for 1 h. Following wash, sections were then incubated in ABC and reacted with the SG/peroxidase kit and mounted on gelatin-subbed slides to air-dry overnight. Slides were then counterstained with Neutral Red, dehydrated, and cover-slipped. In a previous study using the same antibodies, western blots were used to examine antibody specificity in the related Tokay gecko (Yan et al, 2010). In the gecko, blots with CB and PV showed a major band at an estimated molecular weight of 28 and 15 kDa, respectively, similar to the measurement in other species (CB: Ellis et al., 1991; PV: Celio, 1990; Lohmann & Friauf, 1996).

To optimize staining patterns, we incubated cerebellar tissue in the presence or absence of primary antibodies. Purkinje cells were immunoreactive to CB and PV primary antibodies, and were not stained in their absence (Basianelli, 2003). Serial dilutions of primary antibodies from 1:500 to 1:5000 were used to optimize the working concentration of each antibody. We measured the optical density of the labeled neurons in relation to antibody dilution and selected an antibody concentration of 1:1000 because it was in the linear stage of the optical density versus concentration plot.

2.4 | Histology

Two snakes were processed for Nissl staining. After fixation, cryoprotection, and sectioning the brain as described above, sections were mounted on gelatin-subbed slides and air-dried overnight. Slides were then stained with cresyl violet, dehydrated, and coverslipped. A third snake was used for plastic embedding in order to visualize myelinated auditory nerve fibers. After anesthesia, this snake was perfused transcardially with 2% electron microscope (EM) grade paraformaldehyde and 2% EM-grade glutaraldehyde in 0.13 M phosphate buffer (pH 7.4). Following 24 h postfix of the snake's head, the brain was removed and sectioned with a vibratome at 100 μm. The basilar papilla and its connecting nerve were also carefully removed. The tissue was fixed in 1% osmium tetroxide, washed with 0.05 M maleate buffer (pH 5.2), dehydrated, and embedded in Epon araldite 502 (Electron Microscopy Sciences, Hatfield, PA, USA). The papillar nerve containing preganglionic fibers was sectioned orthogonal to the nerve root at 1 μm thickness, and the brain and postganglionic fibers were sectioned in the transverse plane of the brain, oblique to the long axis of the axons. Sections were mounted on glass slides and stained with toluidine blue.

2.5 | Anatomical analyses

Brainstem auditory nuclei were identified based on physical location and projection pattern. Labeled neurons, terminals, and axons were visualized, photographed, and traced with Neurolucida (MBF Bioscience, Williston, VT, USA) in conjunction with a light microscope (Olympus BX60). Nuclear volume and morphometrics of neurons and terminals were quantified with Neurolucida Explorer (MBF Bioscience). From BDA-labeled sections, random nonoverlapping locations were selected within the borders of the cochlear nuclei and the area of every terminal in each region of interest was measured at 1000×.

The number of neurons was counted by first drawing a contour around the cochlear nucleus and then placing a marker on every neuron with a clear nucleolus within the nuclear boundaries, thereby counting every neuron. We counted the total population of neurons instead

of obtaining an estimate using stereological protocols because the volume of NM was small. To evaluate the feasibility of using a stereological estimate, we first calculated the average sampling fraction (asf) using the equation asf = area of counting frame/area of sampling grid. In a given section, the total area of NM often fits within the size of the counting frame, and the area of the counting frame and the area of the sampling grid are similar in size. Hence, in the case of counting NM neurons, asf is approximately 1, requiring sampling of 100% of each section. In other words, the total population of NM neurons must be counted instead of estimated from stereology. To ensure the same methods were used for counting NM and NA, we decided to count, instead of estimate, the total population of NA neurons. We were aware that errors arising from split nucleoli might cause overestimation and should be corrected by an equation from Abercrombie (1946): $N_{real} = N_{counted} \times T/(T + h)$, where T is the thickness of the section and h is the thickness of the nucleoli. However, since the section thickness was 50 μm, which greatly exceeds the typical maximum dimension of nucleoli, $T/(T + h)$ approaches 1.

Morphometrics of neurons were measured at the plane where a clear nucleolus could be seen. The form factor of neurons was defined as the area of the neuron profile divided by the area of a circle having the same perimeter, calculated as ($4\pi \times$ area/perimeter^2). As the contour of the neuron approaches a perfect circle, the value approaches 1. The total number of auditory nerve fibers was counted by placing a marker on every axon in a single cross section of the preganglionic papillar nerve. The mean diameter of preganglionic fibers was quantified by measuring cross sections of every axon in MyelTracer (Kaiser et al., 2021) as equivalent circle diameter (ECD), calculated from $2\sqrt{(\text{area}/\pi)}$. While the plane of section was orthogonal to the nerve root, note that use of ECD may overestimate the axon diameter if the plane of section deviates from a perfect cross section. Postganglionic fiber diameters were obtained from transverse sections that contained obliquely cut fibers, and in these cases the largest minor axis of the ellipse was measured in ImageJ (NIH). Measurements of the postganglionic axon diameter were obtained from all visible axons in a single 1-μm semithin transverse brain section. The g-ratio was calculated as the ratio between the inner axon diameter and the outer axon diameter that included myelin.

3 | RESULTS

3.1 | Vibrogram

The vibration thresholds of western rat snakes followed a U-shaped curve (n = 5 for 20 and 35 Hz stimuli, n = 12 for all other frequencies tested; Figure 3), with best frequencies between 50 Hz (-29.6 ± 2.4 dB re. ms^{-2}) and 100 Hz (-29.2 ± 3.2 dB re. ms^{-2}). The latency of the evoked potential response from the click stimulus onset was 4.6 ± 0.8 ms at 21°C (n = 12; Figure 2b). Vibration sensitivity was similar for 20 and 35 Hz, increased at 50 and 100 Hz, and declined rapidly at frequencies above 100 Hz. All thresholds measured were at least 20 dB above the total octave noise.

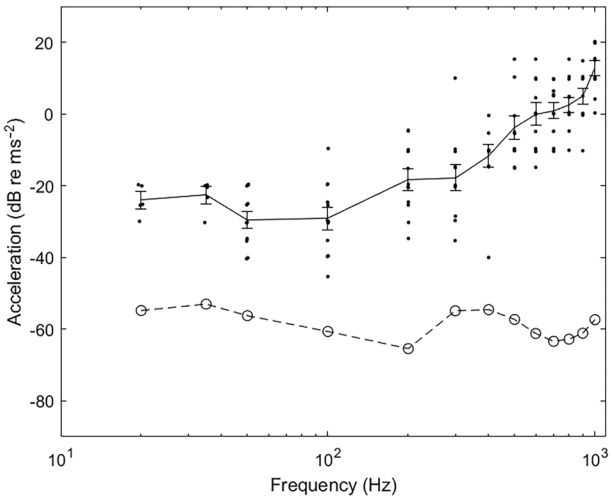

FIGURE 3 Vibrogram of the western rat snake. Detection thresholds are plotted as mean ± *SEM*. Individual thresholds, •; noise floor, ○. For 20 and 35 Hz, $N = 5$. For all other frequencies tested, $N = 12$.

3.2 | Auditory nerve

The VIIIth nerve is divided into an anterior branch that receives input from the anterior and lateral semicircular canals, saccule and utricle, and a posterior branch that receives input from the posterior semicircular canal, saccule, basilar papilla, and lagena (see Figure 1b,c; Baird, 1970; Wever, 1978). The basilar papilla is recognized as an auditory endorgan in land vertebrates (Fritzsch et al., 2013; Walton et al., 2017). BDA crystals placed in the small nerve roots supplying the basilar papilla labeled cell bodies in the dorsal portion of the posterior ganglia. In the brain, the labeled axons in the posterior nerve root bifurcated to form a lateral ascending branch projecting to NA and a more medial descending branch projecting to NM, with NA extending more rostrally and NM extending more caudally (Figure 5a,b). Cochlear nerve fibers projecting to NM mainly traveled ventral to NA. Fibers from the basilar papilla did not project to other hindbrain targets.

We counted 838 fibers from the cross section of the auditory nerve (Figure 4a). Table 1 summarizes the measurements of axon diameters leaving the basilar papilla (Figure 4a; preganglionic), leaving the cochlear ganglia before bifurcation (Figure 4b; postganglionic, prebifurcation) and after bifurcation to innervate the NA (Figure 4c) and NM (Figure 4d), as well as their respective g-ratios. The sites of bifurcation were not visible in the semithin sections. We also could not accurately identify the boundaries of NM. Thus, identification of the postbifurcation fibers was an approximation based on their location in the transverse brain sections. Note that postganglionic fibers were measured from transverse sections of the brain and typically have more variable diameters.

After labeling of the basilar papilla with BDA, bouton terminals were found to be distributed throughout NA and NM. Most bouton terminals were located in the neuropil, with a smaller number of large perisomatic bouton terminals. The mean area of bouton terminals in NA was

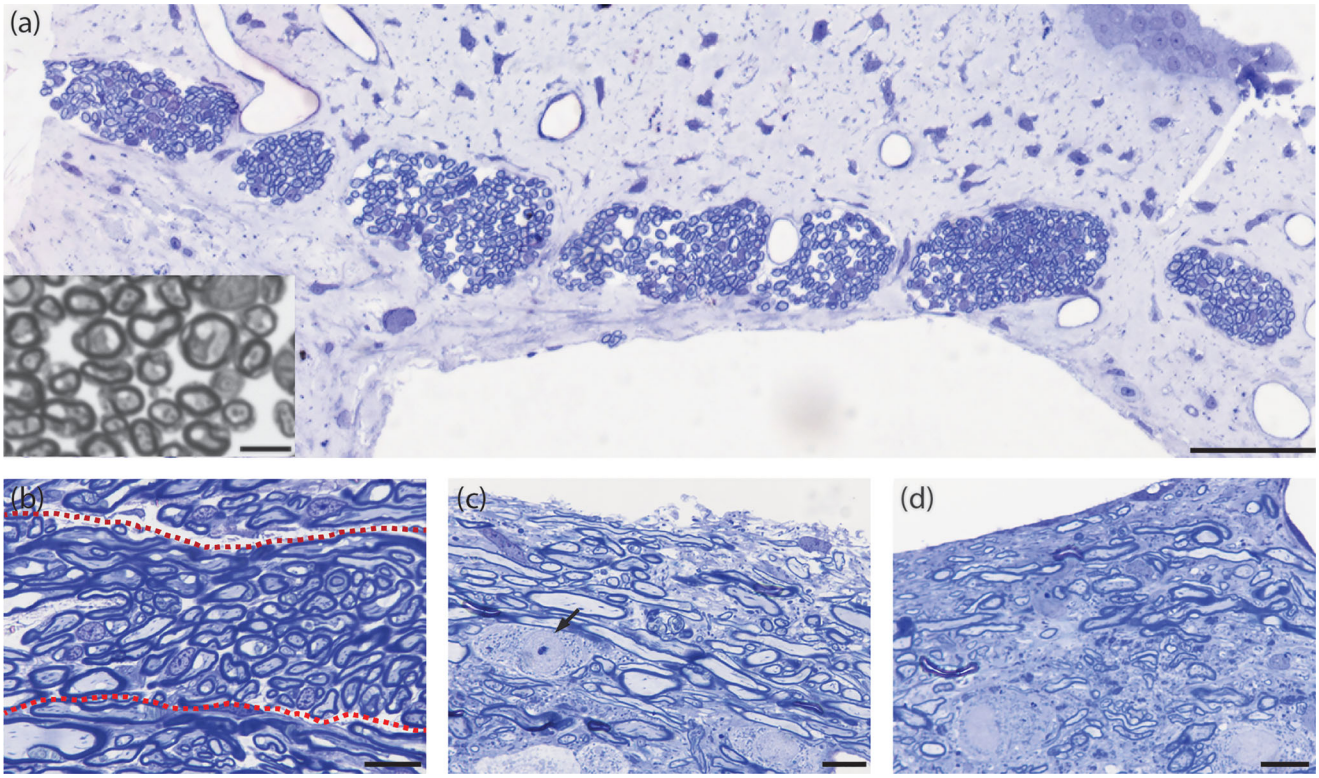

FIGURE 4 Auditory nerve axons. (a) Low-magnification cross sections of the preganglionic papillar nerve. For all photomicrographs, the left side shows medial, right side lateral, top dorsal, and bottom ventral orientation. Scale bar = 50 μm. Inset: Grayscale higher magnification view shows that most fibers are myelinated. Scale bar = 5 μm. (b) Transverse brain sections showing the postganglionic papillar nerve in the dorsal part of the posterior branch of the VIIIth nerve (area in dashed lines). Scale bar = 10 μm. (c) Transverse brain sections showing the papillar nerve collaterals in nucleus angularis (NA). Arrow indicates an NA neuron. Scale bar = 10 μm. (d) Transverse brain sections showing the possible papillar nerve collaterals around nucleus magnocellularis (NM). Scale bar = 10 μm.

2.3 ± 1.3 μm^2 (n = 234, from three snakes) and the mean area of bouton terminals in NM was 1.4 ± 1.0 μm^2 (n = 287, from three snakes). No large lobulated terminals (endbulbs) were observed in the western rat snake NA or NM.

3.3 | Nucleus angularis

NA formed a distinguishable eminence on the dorsal surface of the medulla adjacent to the VIIIth nerve root (Nissl; Figure 6a). Caudally NA extended as a thin layer that impinged upon the ventrally located nucleus vestibularis ovalis and expanded rostrally to end near the cerebellomedullary junction. NA axons, terminals, and neurons were strongly PV positive, and the PV-positive area overlapped with label from papillar nerve projections (Figure 6b). In cresyl violet–stained sections, NA contained large round cells (Figure 6c), small round cells (Figure 6d), and fusiform cells (Figure 6e). Measurements of cell morphometrics are compiled in Table 2. The cell areas of the large round cell type in NA had a large standard deviation, suggesting that this category may be heterogeneous. We did not quantify the respective percentages of each neuron type, but observed that round cells were relatively abundant, whereas fusiform cells were relatively scarce. We counted 580.3 ± 54.3 neurons in NA (average from three animals).

NA was identified by inputs from the basilar papillar nerve branch, its rostral position in the neuraxis, and by projections to the superior olivary nucleus and torus semicircularis. The details of the projections of NA will be described in a later study.

3.4 | Nucleus magnocellularis

NM was located close to the dorsal surface of the brain, above the medial vestibular nucleus. In transverse sections, NM occupied a smaller area than NA and, in contrast to NA, did not form a distinguishable eminence. CB immunohistochemistry allowed for identification of NM, and serial sections of the CB-ir (CB-immunoreactive) material yielded approximately 40 CB-ir neurons in the location of NM (Figure 7b). Since we were unable to identify nucleoli unambiguously in the immunohistochemical material, the NM cell counts are given as an approximation. NM neurons were also lightly positive for PV.

Because of its small size and low cell count, NM was difficult to detect in the Nissl material (Figure 7a). We were, however, able to use papillar nerve projections to identify the rostral border of NM as medial and caudal to NA. The boundaries between the two nuclei were clearly demarcated (Figure 5 a). The caudal border of NM extended slightly caudal to the VIIIth nerve root. The majority of cells in NM were round,

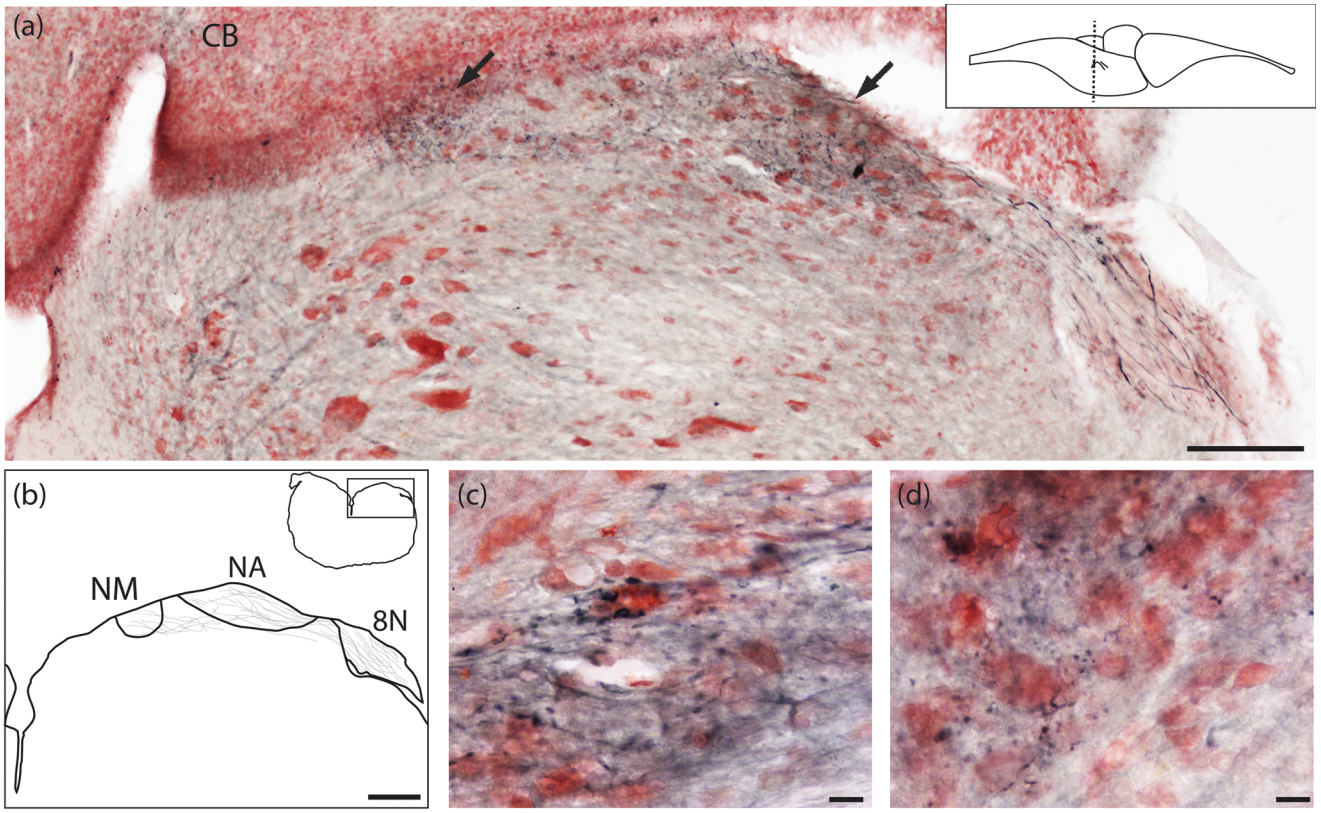

FIGURE 5 Projections of the papillar branch of the VIIIth nerve. (a) Brainstem projections of the auditory branch of the VIIIth nerve. Arrows denoting two terminal fields in nucleus magnocellularis (NM) (left) and nucleus angularis (NA) (right). A small portion of the dorsal brainstem overlaps the cerebellum (CB). Inset: Lateral view showing plane of section. Scale bar = 100 μm. (b) Schematic line drawing of cochlear nuclei based on projections in panel (a). Axons were labeled in gray to show their projection to the cochlear nuclei. 8N, cranial nerve VIII. Scale bar = 100 μm. (c) Terminal field in NA. Scale bar = 10 μm. (d) Terminal field in NM. Compared to the terminal field in NA, most of the bouton terminals were small in NM. Scale bar = 10 μm.

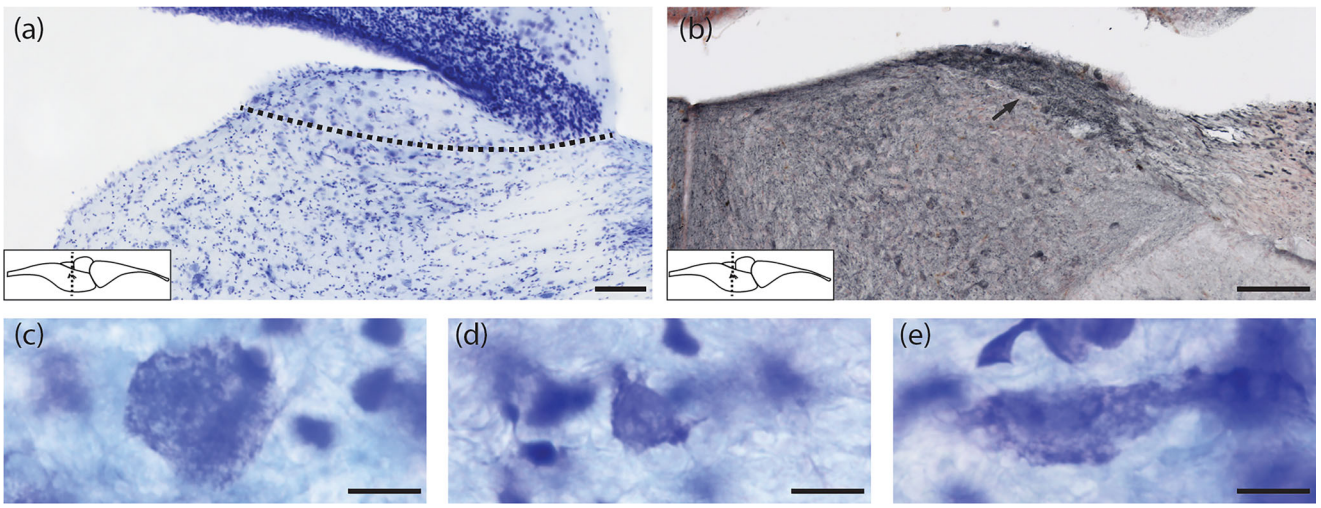

FIGURE 6 Nucleus angularis in the western rat snake. (a) Location and boundaries (dashed line) of nucleus angularis (NA) in the acoustic tubercle, stained with cresyl violet. Inset: Lateral view showing plane of section. Scale bar = 100 μm. (b) Parvalbumin-immunoreactive NA neurons and neuropil (arrow), counterstained with neutral red. Scale bar = 100 μm. (c–e) High-magnification images of Nissl-stained large round (c), small round (d), and fusiform (e) cells in NA. Scale bar = 10 μm.

TABLE 1 Diameter of axons from the basilar papilla.

Location	Number of fibers	Plane of section relative to long axis	Measurement type	Mean diameter (excluding myelin) ± *SD*	Mean diameter (including myelin) ± *SD*	Mean g-ratio ± *SD*
Preganglionic	791	Perpendicular	Equivalent circle diameter	2.2± 0.6	3.3 ± 0.7	0.66 ± 0.07
Postganglionic, prebifurcation	150	Oblique	Minor axis of the ellipse	1.9 ± 0.8	3.0 ± 0.9	0.63 ± 0.09
Postganglionic, postbifurcation, to NA	120	Oblique	Minor axis of the ellipse	1.4 ± 0.8	2.0 ± 0.8	0.67 ± 0.11
Postganglionic, prebifurcation, to NM	150	Oblique	Minor axis of the ellipse	1.0 ± 0.5	1.5 ± 0.6	0.68 ± 0.09

Note: All measurements of fiber diameters (in μm ± *SD*) were obtained from semithin sections viewed with a light microscope at 1000×. Preganglionic fiber diameters were quantified from the cross section of the auditory nerve, while all other measurements were sampled from transverse sections of the brain. Due to the difficulty of discerning cochlear nuclei in the semithin sections, identification of the fibers was based on their approximate location.

TABLE 2 Morphometrics of different neuron types.

Cell type	Sample size	Mean area ± *SD*	Form factor ± *SD*
Nucleus angularis			
Large round	32	142.1 ± 71.2	0.82 ± 0.07
Small round	30	39.8 ± 10.6	0.85 ± 0.04
Fusiform	9	79.1 ± 34.7	0.52 ± 0.06
Nucleus magnocellularis			
Round	51	64.7 ± 22.4	0.81 ± 0.07
Fusiform	15	76.4 ± 26.3	0.54 ± 0.08

Note: Measurements of NA neurons were obtained from Nissl-stained sections from a single animal. Measurements of NM neurons were obtained from CB-ir sections from two animals. Mean areas in μm^2 ± *SD*.

with a smaller population of similarly sized fusiform cells. Measurements of cell morphometrics are compiled in Table 2. NM neurons were measured at maximum diameter in each 50-μm section since nucleoli were difficult to identify in immunostained material.

NM was identified by several features: its caudal position in the neuraxis, the receipt of primary afferent input from the basilar papilla, and lack of projections to the superior olivary nucleus and the torus semicircularis. The details of the projections of NM will be described in a later study.

4 | DISCUSSION

Since the studies of Miller (1980) and Defina (1981), both of whom used anterograde axonal degeneration of the VIIIth nerve, there have been no further attempts to examine the auditory brainstem neuroanatomy in snakes. In the current study, we determined the boundaries, size, and potential connections of the first-order cochlear nuclei of the western rat snake (*P. obsoletus*), using a combination of Nissl staining, tract tracing, and immunohistochemistry. We have also measured the hearing sensitivity of this species.

Despite the absence of tympanic ears, snakes can hear. Vibration-evoked potential recordings demonstrate that the western rat snake has peak sensitivity in the low-frequency range (50–100 Hz), similar to that of other snakes (Christensen et al., 2012; Hartline, 1971). However, the vibration threshold for the western rat snake was about 25 dB higher at the low frequencies, and about 10 dB higher at higher frequencies, than the ball python and rattlesnake (Christensen et al., 2012; Hartline, 1971). This discrepancy may result from differences in methodology. We used isoflurane as the anesthetic agent, while Christensen et al. (2012) and Harline (1971) used ketamine and sodium pentobarbital, respectively. Compared to injection anesthetics, isoflurane has been reported to increase auditory evoked response thresholds in barn owls and rodents (Cederholm et al., 2012; Ruebhausen et al., 2012; Stronks et al., 2010; Thiele & Köppl, 2018). The sensitivity to aerial sound of western rat snakes assessed using cochlear microphonics reported best frequencies around 400 Hz (Wever, 1978), higher

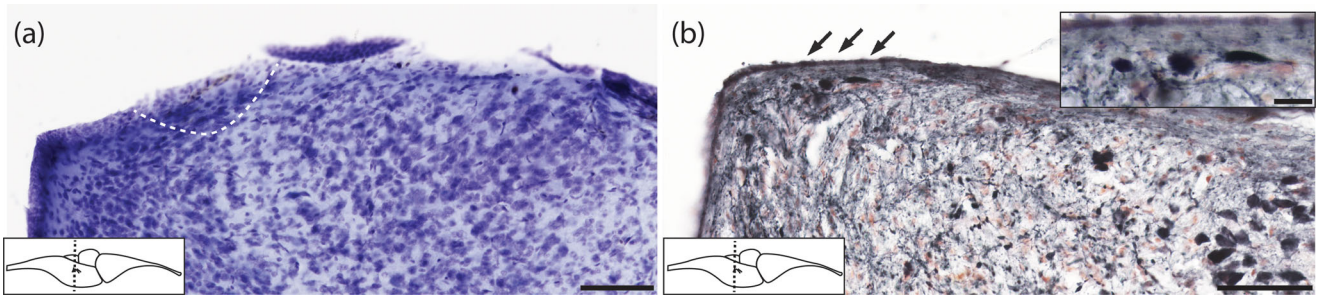

FIGURE 7 Nucleus magnocellularis in the western rat snake. (a) Location of nucleus magnocellularis (NM) (dashed line) corresponding to the area defined in the calbindin-immunoreactive (CB-ir) material and nerve tracing results, stained with cresyl violet. Note the lack of distinct nuclear boundaries in this area. Inset: Lateral view showing plane of section. Scale bar = 100 μm. (b) CB-ir NM neurons (arrows). Scale bar = 100 μm. Inset top right: Magnified view of NM neurons. Note the presence of both round and fusiform cells. Scale bar = 20 μm.

than that in our findings. This discrepancy may be attributed to their low sample size ($n = 2$).

4.1 | The auditory nerve projections are similar to low-frequency fibers in other reptiles

The number of papillar nerve fibers counted in our study (838) was consistent with Miller and Beck (1990), who counted 824 fibers in the same species. Western rat snake auditory nerve fibers were similar in size to other reptiles. For example, the mean diameter of tectorial and free-standing fibers (likely excluding myelin, preganglionic) was 2.81 and 1.97 μm, respectively, in the alligator lizard (Mulroy & Oblak, 1985), comparable to 2.2 μm of the western rat snake. A large-scale survey of auditory nerve fibers (including myelin, preganglionic) in 37 lizards reported that the majority of axon diameters fell in the 2–4 μm range (Miller, 1985), which also overlaps that of the western rat snake (3.3 μm). Similar measurements of preganglionic fibers were found in birds (Köppl, 1997; Köppl et al., 2000). The g-ratio of axons were also comparable to that of birds (Köppl, 1997; Köppl et al., 2000).

Projections from the western rat snake basilar papilla entered the medulla where they bifurcate and terminate in two nonoverlapping nuclei, NA and NM, following the diapsid pattern (Carr, 2020; Walton et al., 2017). These auditory nerve projections were similar to those of lizards, although studies that measured postganglionic nerve fiber diameters from tract tracing material reported larger diameters in alligator lizards and geckos (Szpir et al., 1990; Tang et al., 2012). These differences may arise from methodological variation, since Szpir et al. (1990) measured horseradish peroxidase-labeled fibers in 50-μm thick sections. Tang et al. (2012) found that fibers projecting to NM were thicker than those projecting to NA in the gecko, whereas in the western rat snake, NM collaterals were thinner than NA collaterals. Moreover, in birds, relatively thicker myelination was observed in smaller axons (Köppl et al., 2000); in contrast, the thin NM collaterals of the western rat snake had myelination comparable with the larger diameter NA collaterals.

The terminals of the western rat snake auditory nerve formed round boutons in NM and NA. We found no evidence of the large axosomatic terminals resembling endbulbs of Held that can be found in lizards, birds, alligators, and mammals (Carr & Boudreau, 1991; Carr & Soares, 2002; Szpir et al., 1990; Tang et al., 2012). Endbulb synapses are hypothesized to facilitate phase-locking at high frequencies (Carr et al., 2001; Carr & Soares, 2002; Hong & Sanchez, 2018). Their absence was unsurprising, since the low best frequency region of the barn owl NM (<1 kHz) and the chicken NM (<500 Hz), which overlaps with the vibration detection range of western rat snakes, also receives bouton terminals instead of endbulbs (Fukui & Ohmori, 2004; Köppl, 1994; Wang et al., 2017). Turtles share similar best frequencies with the western rat snake (Christensen-Dalsgaard et al., 2012; Crawford & Fettiplace, 1980), and also do not have large terminals in NM (Willis, 2014), contrary to a prior report (Browner & Marbey, 1988).

4.2 | The location of NA in the western rat snake differs from that of lizards

NA forms a dorsal eminence in the acoustic tubercle adjacent to the VIIIth nerve root in the western rat snake. This corroborates the finding of Weston (1936) in the garter snake (*Thamnophis*), where NA was identified as the only cochlear nucleus. In other studies, it is unclear whether the single auditory nucleus recognized by Holmes (1902), Schwab (1979) and ten Donkelaar and Nieuwenhuys (1979) was NA. It is possible that a dorsal eminence consisting of only NA does not translate to other snake species (see discussion below on NM). Nevertheless, NA is well-developed in the western rat snake, and has a similar number of cells to the alligator lizard NA, with 618 neurons (Szpir et al., 1995) versus 580 in the western rat snake NA.

The western rat snake NA is located more laterally than NA in lizards. In lizards, NA is separated into medial and lateral divisions, with medial NA located close to the medial surface of the acoustic tubercle (Barbas-Henry & Lohman, 1988; Foster & Hall, 1978; Miller, 1975; Szpir et al., 1990; Tang et al., 2012). The medial division of NA is the only region of the first-order nuclei to receive inputs from the specialized high-frequency areas of the basilar papilla with bidirectionally oriented hair cells (Köppl & Manley, 1992; Manley, 2002; Miller, 1992; Szpir et al., 1990, 1995). The snake basilar papilla, however, does not have specialized high-frequency areas and only houses unidirectional hair cells (Manley, 2002; Miller, 1978, 1980; Miller & Beck, 1990).

Its projections to NA terminate laterally. The most parsimonious explanation for the difference in NA's location is that ancestral snakes secondarily lost the medial high-frequency regions in the squamate basilar papilla, likely related to the loss of their tympanic middle ear (Manley, 2017). NA is also located laterally in archosaurs including birds and crocodilians (Köppl, 2001; Leake, 1974; Soares & Carr, 2001). Considering the early divergence of lepidosaurs and archosaurs (Ezcurra et al., 2014), similarities between the location of the western rat snake NA and the avian NA may reflect the ancestral pattern, and the medial division of NA in lizards is most likely a derived condition related to the specialized high-frequency region of their basilar papilla.

NA contains heterogenous cell types; large cells and small round cells were abundant and fusiform cells rare. Similar heterogenous distributions of cell types characterize the NA divisions in the alligator lizard (Szpir et al., 1995) and the avian NA (Bloom et al., 2014; Häusler et al., 1999; Soares & Carr, 2001).

4.3 | NM is small in the western rat snake

NM in the western rat snake is located medially in the acoustic tubercle and caudal to NA, and its location is consistent with observations from previous literature on snakes, and similar to other reptiles (Carr & Boudreau, 1991; Foster & Hall, 1978; Leake, 1974; Miller, 1975, 1980; Molenaar, 1976; Szpir et al., 1990; Willis & Carr, 2017). While Miller (1980) described NM as consisting of an NM medialis and NM lateralis, he also noted that in *Pituophis catenifer* and *Nerodia sipedon* the two divisions were "not clearly separable," and that NM forms "a cap-like shield over the underlying vestibular nuclei." In the closely related western rat snake, we were also unable to differentiate NM into medial and lateral divisions.

The western rat snake NM is remarkably small, occupying a smaller area than NA in transverse sections, and it does not form a notable dorsal cap. These findings conflict with earlier quantifications of NM and NA in *P. obsoletus* (formerly *Elaphe obsoleta*; DeFina, 1981; Defina & Kennedy, 1983), where NM nuclear volume (0.084 mm^3) exceeded NA volume (0.022 mm^3) in adult animals (average length = 93.1 cm). To compare, in our measurement of an adult animal (case 124, CB-ir, length = 120 cm), the volume of NM was about an order of magnitude smaller than that of NA (NM = 0.004 mm^3, NA = 0.041 mm^3). Moreover, Defina and Kennedy's (1983) average count of 146.2 neurons in NM exceeded our estimate by 3-fold. These discrepancies may arise from the resolution of their methodology; quantitative data by DeFina (1981) and Defina and Kennedy (1983) were largely obtained from Nissl-stained material and VIIIth nerve axonal degeneration. During our study, we found that nuclear boundaries of the western rat snake NM were difficult to delineate solely based on Nissl material (Figure 7a). The method of VIIIth nerve degeneration could also lead to unspecific labeling of adjacent vestibular nuclei. While it is possible that there was heterogenous expression of CB in NM, which would lead to our underestimation of the number of cells in NM, both the neuron number and nuclear volume of NM from our study greatly exceeded that of NA in DeFina (1981) and Defina and Kennedy (1983), which suggests that they, and possibly Miller (1980) who used the same methods, may have overestimated the area of NM in some snake species, including the western rat snake.

The small size of the western rat snake NM was supported not only by visual comparisons but also by cell counts. The alligator lizard NM has 245 neurons (Szpir et al., 1995), and the avian NM typically exceeds 2000 neurons (Winter, 1963; Winter & Schwartzkopff, 1961), both of which are greater than the approximately 40 neurons found in the western rat snake. Auditory specialists have a higher number of cells in the cochlear nuclei compared to nonspecialists (Kubke et al., 2004), and the small number of cells in the western rat snake NM suggests that the western rat snake is not an auditory specialist. Furthermore, the presence of a large NA and a small NM suggests that ascending monaural pathways are more prominent than binaural pathways in this snake. We cautiously avoid generalizing the small size of NM to all snake species, since there is evidence for better developed NM in other snakes (personal observations; Miller, 1980; Molenaar, 1976).

4.4 | Snakes have a central auditory system for processing vibration despite loss of the tympanic middle ear

Although earlier authors have proposed that snakes diverged prior to the appearance of the tympanic middle ear in the lepidosaur lineage, and that the atympanic middle ear in snakes is ancestral (Miller, 1968; Tumarkin, 1955), more recent paleontological evidence, including that from many crown-group lepidosaur fossils, reveals an expanded lateral quadrate concavity (conch) that preceded the divergence of snakes (Evans, 2016; Ford et al., 2021; Simões et al., 2018). These findings support the alternative hypothesis that snakes secondarily lost their tympanic middle ear. Our results suggest that first-order cochlear nuclei remained present despite the loss of an impedance-matching middle ear and tympanum to improve the detection of airborne sound.

Sensitivity of snakes to airborne sound can be explained by sound-induced head vibrations alone (Christensen et al., 2012), which suggests that sound pressure and substrate vibration are both presented to snakes as vibrational stimuli. Therefore, it is reasonable to conclude that snakes, at least to some extent, detect vibrations using the auditory endorgan, the basilar papilla, and centrally process vibrational stimuli in the ascending auditory pathways. While seismic or aquatic vibration are primarily detected by otolithic endorgans such as the saccule in fish and amphibians (Christensen-Dalsgaard & Buhl Jørgensen, 1988; Christensen-Dalsgaard & Carr, 2008; Popper & Fay, 1999), nonotolithic endorgans such as the organ of Corti in mammals and the amphibian papilla in amphibians also facilitate vibration sensing (Capshaw et al., 2022; Christensen-Dalsgaard & Narins, 1993; Stenfelt, 2013; Yu et al., 1991). In snakes, it has been hypothesized that vibrational stimuli impinging on the lower jaw or quadrate may cause movement of the stapes relative to the oval window, causing fluid displacement in the inner ear and stimulation of the basilar papilla (Friedel et al., 2008; Wever, 1978). Currently, parsimony supports

the contribution of auditory pathways to vibration detection; in vivo recordings from the papillar branch of the VIIIth nerve or cochlear nuclei would provide direct evidence. Additionally, we do not rule out the possibility that the saccule, or other otolithic endorgans in the inner ear, may also contribute to the snake's sensitivity to vibration.

Given that the basilar papilla may have evolved only once (for review, see Fritzsch et al., 2013), its appearance would have preceded the evolution of the tympanic middle ear, and there likely existed a period in evolutionary history where tetrapods were atympanic but had basilar papillae. Many early tetrapods, such as *Captorhinus*, possessed stapes coupled to the quadrate bone (and indirectly the lower jaw) similar to the condition in snakes (Clack, 1997; Clack & Anderson, 2016; Sobral et al., 2016). While the ability of a snake-like middle ear for detecting airborne sound was likely poor (Christensen et al., 2012; Hartline, 1971; Hartline & Campbell, 1969), our study suggests that it could potentially stimulate papillar pathways to mediate hearing vibrations in early land vertebrates.

ACKNOWLEDGMENTS

We thank Grace Capshaw, Hilary Bierman, and Edward Smith for their help with experimental setup for evoked potential recordings, Disa Basu for her assistance with immunohistochemistry, and Bruce A. Young for his discussions during experimental planning. We thank Grace Capshaw and Bruce A. Young for their critical reading of the manuscript. This work was partly funded by NIH R01DC019341 to C.E.C.

CONFLICT OF INTEREST STATEMENT

The authors declare no conflicts of interest.

DATA AVAILABILITY STATEMENT

The data that support the findings of this study are available from the corresponding author upon request.

PEER REVIEW

The peer review history for this article is available at https://publons.com/publon/10.1002/cne.25495.

ORCID

Dawei Han https://orcid.org/0000-0001-5557-8051

REFERENCES

Abercrombie, M. (1946). Estimation of nuclear population from microtome sections. *The Anatomical Record*, *94*(2), 239–247.

Auen, E. L., & Langebartel, D. A. (1977). The cranial nerves of the colubrid snakes *Elaphe* and *Thamnophis*. *Journal of Morphology*, *154*(2), 205–222. https://doi.org/10.1002/jmor.1051540203

Ashida, G., & Carr, C. E. (2011). Sound localization: Jeffress and beyond. *Current Opinion in Neurobiology*, *21*(5), 745–751. https://doi.org/10.1016/j.conb.2011.05.008

Baird, I. L. (1970). The anatomy of the reptilian ear. In C. Gans & T. S. Parsons (Eds.), *Biology of the Reptilia, Volume 2: Morphology B* (pp. 193–275). Academic Press.

Barbas-Henry, H. A., & Lohman, A. H. M. (1988). Primary projections and efferent cells of the VIIIth cranial nerve in the monitor lizard, *Varanus exanthematicus*. *Journal of Comparative Neurology*, *277*(2), 234–249. https://doi.org/10.1002/cne.902770206

Bastianelli, E. (2003). Distribution of calcium-binding proteins in the cerebellum. *The Cerebellum*, *2*, 242–262. https://doi.org/10.1080/14734220310022289

Bloom, S., Williams, A., & MacLeod, K. M. (2014). Heterogeneous calretinin expression in the avian cochlear nucleus angularis. *Journal of the Association for Research in Otolaryngology*, *15*(4), 603–620. https://doi.org/10.1007/s10162-014-0453-0

Brandt, C., Andersen, T., & Christensen-Dalsgaard, J. (2007). Demonstration of a portable system for auditory brain- stem recordings based on pure tone masking difference. In T. Dau, J. M. Buchholz, J. M. Harte, & T. U. Christiansen (Eds.), *Auditory signal processing in hearing-impaired listeners., 1st Symposium on Auditory and Audiological Research* (pp. 241–248). Centertryk.

Brandt, C., Brande-Lavridsen, N., & Christensen-Dalsgaard, J. (2018). The masked ABR (mABR): A new measurement method for the auditory brainstem response. *Journal of the Association for Research in Otolaryngology*, *19*(6), 753–761. https://doi.org/10.1007/s10162-018-00696-x

Browner, R. H., & Marbey, D. (1988). The nucleus magnocellularis in the red-eared turtle, *Chrysemys scripta elegans*: Eighth nerve endings and neuronal types. *Hearing Research*, *33*(3), 257–271. https://doi.org/10.1016/0378-5955(88)90156-6

Capshaw, G., Christensen-Dalsgaard, J., & Carr, C. E. (2022). Hearing without a tympanic ear. *Journal of Experimental Biology*, *225*(12), jeb244130. https://doi.org/10.1242/jeb.244130

Capshaw, G., Soares, D., Christensen-Dalsgaard, J., & Carr, C. E. (2020). Seismic sensitivity and bone conduction mechanisms enable extratympanic hearing in salamanders. *Journal of Experimental Biology*, *223*(24), jeb236489. https://doi.org/10.1242/jeb.236489

Carr, C. E. (2020). Evolution of central pathways. In B. Fritzsch (Ed.), *The senses: A comprehensive reference* (2nd ed., Vol. 2, pp. 354–376). Elsevier. https://doi.org/10.1016/b978-0-12-809324-5.24168-0

Carr, C. E., & Boudreau, R. E. (1991). Central projections of auditory nerve fibers in the barn owl. *Journal of Comparative Neurology*, *314*(2), 306–318. https://doi.org/10.1002/cne.903140208

Carr, C. E., Christensen-Dalsgaard, J., Edds-Walton, P., Köppl, C., Tang, Y., Young, B. A., & Willis, K. L. (2016). Evolutionary trends in hearing in non-mammalian vertebrates. In J. H. Kaas (Ed.), *Evolution of nervous systems* (2nd ed., Vol. 1, pp. 291–308). Elsevier. https://doi.org/10.1016/B978-0-12-804042-3.00011-7

Carr, C. E., & Soares, D. (2002). Evolutionary convergence and shared computational principles in the auditory system. *Brain, Behavior and Evolution*, *59*(5–6), 294–311. https://doi.org/10.1159/000063565

Carr, C. E., Soares, D., Parameshwaran, S., & Perney, T. (2001). Evolution and development of time coding systems. *Current Opinion in Neurobiology*, *11*(6), 727–733. https://doi.org/10.1016/S0959-4388(01)00276-8

Cederholm, J. M. E., Froud, K. E., Wong, A. C. Y., Ko, M., Ryan, A. F., & Housley, G. D. (2012). Differential actions of isoflurane and ketamine-based anesthetics on cochlear function in the mouse. *Hearing Research*, *292*(1–2), 71–79. https://doi.org/10.1016/j.heares.2012.08.010

Celio, M. R. (1990). Calbindin D-28k and parvalbumin in the rat nervous system. *Neuroscience*, *35*(2), 375–475.

Christensen, C. B., Christensen-Dalsgaard, J., Brandt, C., & Madsen, P. T. (2012). Hearing with an atympanic ear: Good vibration and poor sound-pressure detection in the royal python, *Python regius*. *Journal of Experimental Biology*, *215*(2), 331–342. https://doi.org/10.1242/jeb.062539

Christensen-Dalsgaard, J., Brandt, C., Willis, K. L., Christensen, C. B., Ketten, D., Edds-Walton, P., Fay, R. R., Madsen, P. T., & Carr, C. E. (2012). Specialization for underwater hearing by the tympanic middle ear of the turtle, *Trachemys scripta elegans*. *Proceedings of the Royal Society B: Biological Sciences*, *279*(1739), 2816–2824. https://doi.org/10.1098/rspb.2012.0290

Christensen-Dalsgaard, J., & Buhl Jørgensen, M. (1988). The response characteristics of vibration-sensitive saccular fibers in the grassfrog, *Rana temporaria*. *Journal of Comparative Physiology A*, *162*(5), 633–638. https://doi.org/10.1007/BF01342638

Christensen-Dalsgaard, J., & Carr, C. E. (2008). Evolution of a sensory novelty: Tympanic ears and the associated neural processing. *Brain Research Bulletin*, *75*(2–4), 365–370. https://doi.org/10.1016/j.brainresbull.2007.10.044

Christensen-Dalsgaard, J., & Narins, P. M. (1993). Sound and vibration sensitivity of VIIIth nerve fibers in the frogs *Leptodactylus albilabris* and *Rana pipiens pipiens*. *Journal of Comparative Physiology A*, *172*(6), 653–662. https://doi.org/10.1007/BF00195391

Clack, J. A. (1997). The evolution of tetrapod ears and the fossil record. *Brain, Behavior and Evolution*, *50*(4), 198–212. https://doi.org/10.1159/000113334

Clack, J. A., & Anderson, J. S. (2016). Early tetrapods: Experimenting with form and function. In J. A. Clack, R. R. Fay, & A. N. Popper (Eds.), *Evolution of the vertebrate ear: Evidence from the fossil record* (pp. 71–105). Springer. https://doi.org/10.1007/978-3-319-46661-3_4

Conlee, J. W., & Parks, T. N. (1986). Origin of ascending auditory projections to the nucleus mesencephalicus lateralis pars dorsalis in the chicken. *Brain Research*, *367*(1-2), 96–113. https://doi.org/10.1016/0006-8993(86)91583-0

Crawford, A. C., & Fettiplace, R. (1980). The frequency selectivity of auditory nerve fibres and hair cells in the cochlea of the turtle. *The Journal of Physiology*, *306*(1), 79–125. https://doi.org/10.1113/jphysiol.1980.sp013387

DeFina, A. V. (1981). *The cochlear nuclei of colubrid and boid snakes* [Doctoral dissertation, New York University]. ProQuest Dissertations and Theses.

Defina, A. V., & Kennedy, M. C. (1983). The cochlear nuclei in colubrid and boid snakes: A qualitative and quantitative study. *Journal of Morphology*, *178*(3), 285–301. https://doi.org/10.1002/jmor.1051780306

Ellis, J. H., Richards, D. E., & Rogers, J. H. (1991). Calretinin and calbindin in the retina of the developing chick. *Cell and Tissue Research*, *264*(2), 197–208.

Evans, S. E. (2016). The lepidosaurian ear: Variations on a theme. In J. A. Clack, R. R. Fay, & A. N. Popper (Eds.), *Evolution of the vertebrate ear: Evidence from the fossil record* (pp. 245–284). Springer. https://doi.org/10.1007/978-3-319-46661-3_9

Ezcurra, M. D., Scheyer, T. M., & Butler, R. J. (2014). The origin and early evolution of Sauria: Reassessing the Permian Saurian fossil record and the timing of the crocodile-lizard divergence. *PLoS ONE*, *9*(2), e89165. https://doi.org/10.1371/journal.pone.0089165

Ford, D. P., Evans, S. E., Choiniere, J. N., Fernandez, V., & Benson, R. B. J. (2021). A reassessment of the enigmatic diapsid *Paliguana whitei* and the early history of Lepidosauromorpha. *Proceedings of the Royal Society B: Biological Sciences*, *288*(1957). https://doi.org/10.1098/rspb.2021.1084

Foster, R. E., & Hall, W. C. (1978). The organization of central auditory pathways in a reptile, *Iguana iguana*. *Journal of Comparative Neurology*, *178*(4), 783–831. https://doi.org/10.1002/cne.901780412

Friedel, P., Young, B. A., & van Hemmen, J. L. (2008). Auditory localization of ground-borne vibrations in snakes. *Physical Review Letters*, *100*(4), 048701. https://doi.org/10.1103/PhysRevLett.100.048701

Fritzsch, B., Pan, N., Jahan, I., Duncan, J. S., Kopecky, B. J., Elliott, K. L., Kersigo, J., & Yang, T. (2013). Evolution and development of the tetrapod auditory system: An organ of Corti-centric perspective. *Evolution and Development*, *15*(1), 63–79. https://doi.org/10.1111/ede.12015

Fukui, I., & Ohmori, H. (2004). Tonotopic gradients of membrane and synaptic properties for neurons of the chicken nucleus magnocellularis. *Journal of Neuroscience*, *24*(34), 7514–7523. https://doi.org/10.1523/JNEUROSCI.0566-04.2004

Grothe, B., Carr, C. E., Casseday, J. H., Fritzsch, B., & Köppl, C. (2004). The evolution of central pathways and their neural processing patterns. In G. A. Manley, A. N. Popper, & R. R. Fay (Eds.), *Evolution of the vertebrate auditory system* (pp. 289–359). Springer. https://doi.org/10.1007/978-1-4419-8957-4_10

Hartline, P. H. (1971). Physiological basis for detection of sound and vibration in snakes. *Journal of Experimental Biology*, *54*(2), 349–371.

Hartline, P. H., & Campbell, H. W. (1969). Auditory and vibratory responses in the midbrains of snakes. *Science*, *163*(3872), 1221–1223. https://doi.org/10.1126/science.163.3872.1221

Häusler, U. H. L., Sullivan, W. E., Soares, D., & Carr, C. E. (1999). A morphological study of the cochlear nuclei of the pigeon (*Columba livia*). *Brain, Behavior and Evolution*, *54*(5), 290–302. https://doi.org/10.1159/000006629

Holmes, G. M. (1902). On the comparative anatomy of the nervus acusticus. *The Transactions of the Royal Irish Academy*, *32*, 101–144.

Hong, H., & Sanchez, J. T. (2018). Need for speed and precision: Structural and functional specialization in the cochlear nucleus of the avian auditory system. *Journal of Experimental Neuroscience*, *12*, https://doi.org/10.1177/1179069518815628

Kaiser, T., Allen, H. M., Kwon, O., Barak, B., Wang, J., He, Z., Jiang, M., & Feng, G. (2021). Myeltracer: A semi-automated software for myelin g-ratio quantification. *eNeuro*, *8*(4), ENEURO.0558–20.2021. https://doi.org/10.1523/ENEURO.0558-20.2021

Kohl, T., Bothe, M. S., Luksch, H., Straka, H., & Westhoff, G. (2014). Organotopic organization of the primary infrared sensitive nucleus (LTTD) in the western diamondback rattlesnake (*Crotalus atrox*). *Journal of Comparative Neurology*, *522*(18), 3943–3959. https://doi.org/10.1002/cne.23644

Köppl, C. (1994). Auditory nerve terminals in the cochlear nucleus magnocellularis: Differences between low and high frequencies. *Journal of Comparative Neurology*, *339*(3), 438–446. https://doi.org/10.1002/cne.903390310

Köppl, C. (1997). Number and axon calibres of cochlear afferents in the barn owl. *Auditory Neuroscience*, *3*, 313–334.

Köppl, C. (2001). Tonotopic projections of the auditory nerve to the cochlear nucleus angularis in the barn owl. *Journal of the Association for Research in Otolaryngology*, *2*(1), 41–53. https://doi.org/10.1007/s101620010027

Köppl, C., & Carr, C. E. (1997). Low-frequency pathway in the barn owl's auditory brainstem. *Journal of Comparative Neurology*, *378*(2), 265–282. https://doi.org/10.1002/(SICI)1096-9861(19970210)378:2(265::AID-CNE9)3.0.CO;2-1

Köppl, C., & Manley, G. A. (1992). Functional consequences of morphological trends in the evolution of lizard hearing organs. In D. B. Webster, A. N. Popper, & R. R. Fay (Eds.), *The evolutionary biology of hearing* (pp. 489–509). Springer. https://doi.org/10.1007/978-1-4612-2784-7_31

Köppl, C., Wegscheider, A., Gleich, O., & Manley, G. A. (2000). A quantitative study of cochlear afferent axons in birds. *Hearing Research*, *139*(1–2), 123–143. https://doi.org/10.1016/S0378-5955(99)00178-1

Kubke, M. F., Massoglia, D. P., & Carr, C. E. (2004). Bigger brains or bigger nuclei? Regulating the size of auditory structures in birds. *Brain, Behavior and Evolution*, *63*(3), 169–180. https://doi.org/10.1159/000076242

Leake, P. A. (1974). Central projections of the statoacoustic nerve in *Caiman crocodilus*. *Brain, Behavior and Evolution*, *10*(1–3), 170–196. https://doi.org/10.1159/000124311

Lohmann, C., & Friauf, E. (1996). Distribution of the calcium-binding proteins parvalbumin and calretinin in the auditory brainstem of adult and developing rats. *Journal of Comparative Neurology*, *367*(1), 90–109.

Manley, G. A. (2002). Evolution of structure and function of the hearing organ of lizards. *Journal of Neurobiology*, *53*(2), 202–211. https://doi.org/10.1002/neu.10115

Manley, G. A. (2017). Comparative auditory neuroscience: Understanding the evolution and function of ears. *Journal of the Association for Research in Otolaryngology*, *18*(1), 1–24. https://doi.org/10.1007/s10162-016-0579-3

McCormick, C. A. (1999). Anatomy of the central auditory pathways of fish and amphibians. In R. R. Fay & A. N. Popper (Eds.), *Comparative hearing:*

Fish and amphibians (pp. 155–217). Springer. https://doi.org/10.1007/978-1-4612-0533-3_5

Miller, M. R. (1968). The cochlear duct of snakes. *Proceedings of the California Academy of Sciences*, *35*(19), 425–476.

Miller, M. R. (1975). The cochlear nuclei of lizards. *Journal of Comparative Neurology*, *159*(3), 375–406. https://doi.org/10.1002/cne.901590306

Miller, M. R. (1978). Scanning electron microscope studies of the papilla basilaris of some turtles and snakes. *American Journal of Anatomy*, *151*(3), 409–435. https://doi.org/10.1002/aja.1001510306

Miller, M. R. (1980). The cochlear nuclei of snakes. *Journal of Comparative Neurology*, *192*(4), 717–736. https://doi.org/10.1002/cne.901920407

Miller, M. R. (1985). Quantitative studies of auditory hair cells and nerves in lizards. *Journal of Comparative Neurology*, *232*(1), 1–24. https://doi.org/10.1002/cne.902320102

Miller, M. R. (1992). The evolutionary implications of the structural variations in the auditory papilla of lizards. In J. F. Webb, A. N. Popper, & R. R. Fay (Eds.), *The evolutionary biology of hearing* (pp. 463–487). Springer. https://doi.org/10.1007/978-1-4612-2784-7_30

Miller, M. R., & Beck, J. (1990). Further serial transmission electron microscopy studies of auditory hair cell innervation in lizards and in a snake. *American Journal of Anatomy*, *188*(2), 175–184. https://doi.org/10.1002/aja.1001880207

Molenaar, G. J. (1976). The rhombencephalon of *Python reticulatus*, a snake possessing infrared receptors. *Netherlands Journal of Zoology*, *27*(2), 133–181. https://doi.org/10.1163/002829677x00018

Mulroy, M. J., & Oblak, T. G. (1985). Cochlear nerve of the alligator lizard. *Journal of Comparative Neurology*, *233*, 463–472.

Popper, A. N., & Fay, R. R. (1999). The auditory periphery in fishes. In R. E. Fay & A. N. Popper (Eds.), *Comparative hearing: Fish and amphibians* (pp. 43–100). Springer. https://doi.org/10.1007/978-1-4612-0533-3_3

Rasmussen, G. L. (1961). A method of staining the statoacoustic nerve in bulk with Sudan black B. *The Anatomical Record*, *139*(4), 465–469.

Ruebhausen, M. R., Brozoski, T. J., & Bauer, C. A. (2012). A comparison of the effects of isoflurane and ketamine anesthesia on auditory brainstem response (ABR) thresholds in rats. *Hearing Research*, *287*(1–2), 25–29. https://doi.org/10.1016/j.heares.2012.04.005

Schwab, M. E. (1979). Variation in the rhombencephalon. In C. Gans, R. G. Northcutt, & P. S. Ulinski (Eds.), *Biology of the Reptilia*, *Volume 10: Neurology B* (pp. 200–246). Academic Press.

Simões, T. R., Caldwell, M. W., Tałanda, M., Bernardi, M., Palci, A., Vernygora, O., Bernardini, F., Mancini, L., & Nydam, R. L. (2018). The origin of squamates revealed by a Middle Triassic lizard from the Italian Alps. *Nature*, *557*(7707), 706–709. https://doi.org/10.1038/s41586-018-0093-3

Soares, D., & Carr, C. E. (2001). The cytoarchitecture of the nucleus angularis of the barn owl (*Tyto alba*). *Journal of Comparative Neurology*, *429*(2), 192–205. https://doi.org/10.1002/1096-9861(20000108)429:2(192::AID-CNE2)3.0.CO;2-5

Sobral, G., Reisz, R., Neenan, J. M., Müller, J., & Scheyer, T. M. (2016). Basal Reptilians, marine Diapsids, and turtles: The flowering of reptile diversity. In J. A. Clack, R. R. Fay, & A. N. Popper (Eds.), *Evolution of the vertebrate ear: Evidence from the fossil record* (pp. 207–243). Springer. https://doi.org/10.1007/978-3-319-46661-3_8

Stenfelt, S. (2013). Bone conduction and the middle ear. In S. Puria, R. Fay, & A. Popper (Eds.), *The middle ear* (pp. 135–169). Springer. https://doi.org/10.1007/978-1-4614-6591-1_6

Stronks, H. C., Aarts, M. C. J., & Klis, S. F. L. (2010). Effects of isoflurane on auditory evoked potentials in the cochlea and brainstem of guinea pigs. *Hearing Research*, *260*(1–2), 20–29. https://doi.org/10.1016/j.heares.2009.10.015

Szpir, M. R., Sento, S., & Ryugo, D. K. (1990). Central projections of cochlear nerve fibers in the alligator lizard. *Journal of Comparative Neurology*, *295*(4), 530–547. https://doi.org/10.1002/cne.902950403

Szpir, M. R., Wright, D. D., & Ryugo, D. K. (1995). Neuronal organization of the cochlear nuclei in alligator lizards: A light and electron microscopic investigation. *Journal of Comparative Neurology*, *357*(2), 217–241. https://doi.org/10.1002/cne.903570204

Takahashi, T. T., & Konishi, M. (1988a). Projections of nucleus angularis and nucleus laminaris to the lateral lemniscal nuclear complex of the barn owl. *Journal of Comparative Neurology*, *274*(2), 212–238. https://doi.org/10.1002/cne.902740207

Takahashi, T. T., & Konishi, M. (1988b). Projections of nucleus angularis and nucleus laminaris to the lateral lemniscal nuclear complex of the barn owl. *Journal of Comparative Neurology*, *274*(2), 212–238. https://doi.org/10.1002/cne.902740207

Tang, Y., Christensen-Dalsgaard, J., & Carr, C. E. (2012). Organization of the auditory brainstem in a lizard, *Gekko gecko*. I. Auditory nerve, cochlear nuclei, and superior olivary nuclei. *Journal of Comparative Neurology*, *520*(8), 1784–1799. https://doi.org/10.1002/cne.23013

ten Donkelaar, H. J., & Nieuwenhuys, R. (1979). The brainstem. In C. Gans, R. G. Northcutt, & P. S. Ulinski (Eds.), *Biology of the Reptilia*, *Volume 10: Neurology B* (pp. 133–200). Academic Press.

Thiele, N., & Köppl, C. (2018). Gas anesthesia impairs peripheral auditory sensitivity in Barn Owls (*Tyto alba*). *eNeuro*, *5*(5), ENEURO.0140–18.2018. https://doi.org/10.1523/ENEURO.0140-18.2018

Tumarkin, A. (1955). On the evolution of the auditory conducting apparatus: A new theory based on functional considerations. *Evolution*, *9*(3), 221–243.

Uetz, P., Freed, P., Aguilar, R., Reyes, F., & Hošek, J. (2023). *The Reptile Database*. http://www.reptile-database.org accessed May 9, 2023

Walton, P. L., Christensen-Dalsgaard, J., & Carr, C. E. (2017). Evolution of sound source localization circuits in the nonmammalian vertebrate brainstem. *Brain, Behavior and Evolution*, *90*(2), 131–153. https://doi.org/10.1159/000476028

Wang, X., Hong, H., Brown, D. H., Sanchez, J. T., & Wang, Y. (2017). Distinct neural properties in the low-frequency region of the chicken cochlear nucleus magnocellularis. *eNeuro*, *4*(2), ENEURO.0016–17.2017. https://doi.org/10.1523/ENEURO.0016-17.2017

Weston, J. K. (1936). The reptilian vestibular and cerebellar gray with fiber connections. *Journal of Comparative Neurology*, *65*(1), 93–199. https://doi.org/10.1002/cne.900650110

Wever, E. G. (1978). *The reptile ear*. Princeton University Press.

Willis, K. L. (2014). *Anatomical and physiological characterization of the turtle brain stem auditory circuit* [Doctoral dissertation, University of Maryland]. ProQuest Dissertations and Theses.

Willis, K. L., & Carr, C. E. (2017). A circuit for detection of interaural time differences in the nucleus laminaris of turtles. *Journal of Experimental Biology*, *220*(22), 4270–4281. https://doi.org/10.1242/jeb.164145

Winter, P. (1963). Vergleichende qualitative und quantitative untersuchungen an der hörbahn von vögeln. *Zeitschrift Für Morphologie Und Ökologie Der Tiere*, *52*(4), 365–400. https://doi.org/10.1007/BF00408568

Winter, P., & Schwartzkopff, J. (1961). Form und Zellzahl der akustischen Nervenzentren in der Medulla oblongata von Eulen (Striges). *Experientia*, *17*(11), 515–516. https://doi.org/10.1007/BF02158630

Yan, K., Tang, Y. Z., & Carr, C. E. (2010). Calcium-binding protein immunoreactivity characterizes the auditory system of *Gekko gecko*. *Journal of Comparative Neurology*, *518*(17), 3409–3426.

Yu, X., Lewis, E. R., & Feld, D. (1991). Seismic and auditory tuning curves from bullfrog saccular and amphibian papular axons. *Journal of Comparative Physiology A*, *169*(2), 241–248. https://doi.org/10.1007/BF00215871

How to cite this article: Han, D., & Carr, C. E. (2023). Central projections of auditory nerve fibers in the western rat snake (*Pantherophis obsoletus*). *Journal of Comparative Neurology*, *531*, 1261–1273. https://doi.org/10.1002/cne.25495